Overexpressed lncRNA FTX promotes the cell viability, proliferation, migration and invasion of renal cell carcinoma via FTX/miR-4429/UBE2C axis

ZHIPING CHEN[1], MENGTING ZHANG[2], YUKANG LU[2], TAO DING[1], ZHANYU LIU[1],
YANMEI LIU[1], ZHAOLING ZHOU[1] and LANFENG WANG[3]

[1]Department of Laboratory Medicine, First Affiliated Hospital of Gannan Medical University;
[2]Department of The First Clinical Medical College, Gannan Medical University; [3]Department of Nephrology,
First Affiliated Hospital of Gannan Medical University, Zhanggong, Ganzhou, Jiangxi 341000, P.R. China

Abstract. The present study aimed to explore the role of long non-coding (lnc)RNA FTX and ubiquitin-conjugating enzyme E2C (UBE2C) in promoting the progression of renal cell carcinoma (RCC) and the underlying regulatory mechanism. Relative levels of lncRNA FTX, UBE2C, AKT, CDK1 and CDK6 in RCC cell lines were detected by reverse transcription-quantitative (RT-q). Expression levels of UBE2C, phosphorylated (p)-AKT/AKT, p-CDK1/CDK1 and p-CDK6/CDK6 in RCC and paracancerous specimens and RCC cells were measured by western blot or immunohisto-chemistry assay. In addition, the proliferative rate, cell viability, cell cycle progression, migratory rate and invasive rate of RCC cells overexpressing lncRNA FTX by lentivirus transfection were determined by a series of functional experiments, including the colony formation assay, MTT assay, flow cytometry, Transwell assay and wound healing assay. The targeted binding relationship in the lncRNA FTX/miR-4429/UBE2C axis was validated by dual-luciferase reporter assay. By intervening microRNA (miR)-4492 and UBE2C by the transfection of miR-4429-mimics or short interfering UBE2C-2, the regulatory effect of lncRNA FTX/miR-4429/UBE2C axis on the progression of RCC was evaluated. Finally, a xenograft model of RCC in nude mice was established by subcutaneous implantation, thus evaluating the *in vivo* function of lncRNA FTX in the progression of RCC. The results showed that lncRNA FTX and UBE2C were upregulated in RCC specimens and cell lines. The overexpression of lncRNA FTX in RCC cells

upregulated UBE2C. In addition, the overexpression of lncRNA FTX promoted the cell viability and proliferative, migratory and invasive capacities of RCC cells and accelerated the cell cycle progression. A dual-luciferase reporter assay validated that lncRNA FTX exerted the miRNA sponge effect on miR-4429, which was bound to UBE2C 3'UTR. Knockdown of UBE2C effectively reversed the regulatory effects of overexpressed lncRNA FTX on the abovementioned phenotypes of RCC cells. In the xenograft model of RCC, the mice implanted with RCC cells overexpressing lncRNA FTX showed a larger tumor size and higher tumor weight than those of controls, while the *in vivo* knockdown of UBE2C significantly reduced the size of RCC lesions, indicating the reversed cancer-promoting effect of lncRNA FTX. Overall, the present study showed that lncRNA FTX was upregulated in RCC and could significantly promote the proliferative, migratory and invasive capacities, enhancing the viability and accelerating the cell cycle progression of RCC cells by exerting the miRNA sponge effect on miR-4429 and thus upregulating UBE2C. lncRNA FTX and UBE2C are potential molecular biomarkers and therapeutic targets of RCC.

Introduction

Renal cancer is among the top ten malignant tumors in the world, with 400,000 newly diagnosed cases annually (1). Renal cell carcinoma (RCC) is a malignant tumor that originates in the renal tubular epithelium, accounting for >90% of renal cancer cases (2) and its incidence has gradually increased in recent years (3). Although great strides have been made on medical techniques where local RCC can be surgically resected with a five-year overall survival of 76% (4), health management of metastatic RCC is quite challenging in clinical practice (5). The occurrence and development mechanism of RCC is closely linked to the epigenetics, tumor heterogeneity and carcinogenesis, immune infiltration and microenvironment (6), with ~3% of cases having a family history (7). A number of genes perform an abnormal expression in RCC, such as the von Hippel-Lindau (VHL), which is often inactivated in sporadic RCC by mutation or promoter hypermethylation (8),

Correspondence to: Professor Lanfeng Wang, Department of Nephrology, First Affiliated Hospital of Gannan Medical University, 23 Qingnian Road, Zhanggong, Ganzhou, Jiangxi 341000, P.R. China
E-mail: czp15083737280@163.com

and BAP-1, which has important implications for utilization of molecular testing, prognosis, future therapeutics and distinguishing clear cell (cc)RCC from other RCC (8,9). Therefore, early diagnosis and active development of effective therapeutic targets have great significance to the research and clinical diagnosis and treatment of RCC.

lncRNAs are noncoding RNAs >200 nucleotides long, serving as key regulators in the physiological and pathological processes of human beings (10). Increasing amounts of evidence has shown that abnormally expressed lncRNAs in RCC are crucially involved in cancer development and progression (11-14). lncRNA FTX is upregulated in adenocarcinoma and gastric cancer, indicating that lncRNA FTX is an oncogene (15,16). He *et al* (17) report that lncRNA FTX is upregulated in RCC as an oncogene and its knockdown inhibits the migratory and invasive capacities of RCC cells. However, the specific molecular mechanism of lncRNA FTX in the malignant progression of RCC remains to be elucidated.

Ubiquitin conjugating enzyme E2 C (UBE2C) is a component of the ubiquitin proteasome system. As an essential factor of the cell cycle regulatory E3, human anaphase promoting complex/cyclosome (APC/C), UBE2C participates in the ubiquitination modification of cyclins and mitosis-related factors, thereby accelerating cell mitosis (18). Previous studies have shown that the mRNA or protein level of UBE2C is abnormally upregulated in a number of types of cancers with poor clinical outcomes, including liver cancer, lung cancer, gastric cancer, colon cancer and cervical cancer (19). UBE2C is a vital gene involved in the development of RCC and is significant to mediate the proliferation and migration of RCC cells (20). However, the molecular mechanism between lncRNA FTX and UBE2C in regulating the development of RCC remains to be elucidated.

In the present study, by detecting the expression levels of lncRNA FTX in the clinical specimens of RCC, it was found that FTX was significantly upregulated. Furthermore, lncRNA FTX was predicted using the StarBase to exert the miRNA sponge effect on miR-4429 to upregulate UBE2C. The present study further analyzed the *in vitro* and *in vivo* functions of lncRNA FTX in RCC by intervening the expression levels of lncRNA FTX, miR-4429 and UBE2C in RCC cells and establishing a xenograft model of RCC in nude mice to explore the potential signaling and mechanisms of lncRNA FTX/miR-4429/UBE2C axis.

Materials and methods

Sample collection. A total of six pairs of RCC and paracancerous specimens that were ≤4 cm away from the margin of RCC lesions were collected from patients with RCC (male to female ratio: 2:1) who were surgically treated in the First Affiliated Hospital of Gannan Medical University. All were patients with RCC hospitalized in the First Affiliated Hospital of Gannan Medical University hospital between March and June 2020 and aged 48-60 years-old, with the median as 53. Renal cancer tissues and adjacent tissues were removed after surgical treatment without radiotherapy or chemotherapy. The fresh tissues were immediately stored in liquid nitrogen and stored in a refrigerator at -80°C after removal and then used for reverse transcription-quantitative (RT-q) PCR, western

blotting or immunohistochemistry (IHC). The specimens were fixed in 4% paraformaldehyde for 24 h at a room temperature and dehydrated and transparentized with gradient concentrations (30, 50, 75, 95 and 100%) of ethanol and xylene, and then embedded in paraffin at 55°C to prepare 4-μm tissue sections. and some fresh specimens were subjected to the isolation of total RNA and proteins for RT-qPCR and western blotting, respectively. The present study was approved by Ethics Review Committee of Scientific Research of Gannan Medical College (number 2020075). All patients who participated were informed of the content of the study and their written informed consent was obtained.

Cell culture. RCC cell lines, including A498 (cat. no. BNCC338630; BeNa Culture Collection), A704 (cat. no. BNCC342393; BeNa Culture Collection), SN12C (cat. no. BNCC341858; BeNa Culture Collection), 769-P (cat. no. BNCC101643; BeNa Culture Collection), the human renal fibroblast cell line KFB (cat. no. HTX2520; Otwo Biotech), human proximal convoluted tubular cell line HK-2 (cat. no. BNCC338012; BeNa Culture Collection) and the 293T cell line (cat. no. MZ-0005; Ningbo Mingzhou Biotechnology Co., Ltd.) were used. Briefly, the cells were seeded in a 10-mm culture dish and cultivated in DMEM (Gibco; Thermo Fisher Scientific, Inc.) supplemented with 10% FBS (Gibco; Thermo Fisher Scientific, Inc.) and 1% penicillin and streptomycin in a humidified incubator containing 5% CO_2 and 95% air at 37°C. The culture medium was replaced every 2 days. Cell passage was conducted using trypsin at over 80% of confluence.

Cell transfection. miR-4429-mimics (5'-AAAAGCUGG GCUGAGAGGCG-3') and mimic-negative control (NC; 5'-AAGUGUCACCGAUUCAAGACG-3'; RiboBio Co., Ltd., Guangzhou, China) and shUBE2C-1, shUBE2C-2, shUBE2C-3 and the empty vector was used as a shNC (Shanghai GeneChem Co., Ltd.) were used in cell transfection performed following the recommendations of Lipofectamine® 2000 reagent (Invitrogen; Thermo Fisher Scientific, Inc.). Briefly, the cells were seeded in a 12-well plate at a density of 5x10⁴ cells/well and cultured to 80% of confluence. After 4-h starvation in serum-free DMEM (Gibco; Thermo Fisher Scientific), 100 nM miR-4429-mimics, mimic-NC or 2 μg shUBE2C was incubated with Lipofectamine® 2000 reagent (Invitrogen; Thermo Fisher Scientific, Inc.) for 20 min, followed by incubation with cells for 40 min at a room temperature. Fresh serum-containing DMEM (Gibco; Thermo Fisher Scientific) was replaced at 24 h and the transfection efficacy was evaluated by RT-qPCR.

RT-qPCR. The cells were cultured at 80% of confluence for RNA extraction. RNA extraction, cDNA synthesis and qPCR were all performed according to the manufacturer's protocols. Briefly, the total RNAs in cells were isolated using TRIzol® (Thermo Fisher Scientific, Inc.) and 1 μg of the total RNA was reversely transcribed to cDNA using a Takara PrimeScript RT reagent kit. Subsequently, qPCR was performed using a SYBR Premix Ex Taq II with Tli RNaseH (Takara Bio, Inc.) on an ABI Prism 7500 system (Thermo Fisher Scientific, Inc.). In brief, the total RNA induced with gDNA eraser and reversely transcribed to cDNA in 42°C for 15 min and then subjected to thermal cycles at 95°C for 15 min, followed by 40 cycles at 95°C for

Table I. Sequences of primers used.

Genes	Sequences
lncRNA FTX-F	5'-GTGTCTCTCTCTCTCTCTCTCTT-3'
lncRNA FTX-R	5'-CCTCTTCAGCAGTAGCATAGTT-3'
miR-4429-F	5'-GGGAGAAAAGCTGGGCTGAG-3'
miR-4429-R	5'-GGCCAGGCAGTCTGAGTTG-3'
UBE2C-F	5'-CTGCCGAGCTCTGGAAAAAC-3'
UBE2C-R	5'-AGGAAAAATTAAAAAGACGACACAAG-3'
Akt-F	5'-CCTGAAGCTACTGGGCAAGGG-3'
Akt-R	5'-ACAAAGCAGAGGCGGTCGTG-3'
CDK1-F	5'-CCTAGCATCCCATGTCAAAAACTTGG-3'
CDK1-R	5'-TGATTCAGTGCCATTTTGCCAGA-3'
CDK6-F	5'-TGCACAGTGTCACGAACAGA-3'
CDK6-R	5'-ACCTCGGAGAAGCTGAAACA-3'
GAPDH-F	5'-AGAAGGCTGGGGCTCATTTG-3'
GAPDH-R	5'-AGGGGCCATCCACAGTCTTC-3'
U6-F	5'-CTCGCTTCGGCAGCACA-3'
U6-R	5'-AACGCTTCACGAATTTGCGT-3'

lncRNA, long non-coding RNA; miR, microRNA; UBE2C, ubiquitin-conjugating enzyme E2C; F, forward; R, reverse.

5 sec, 60˚C for 30 sec and 72˚C for 40 sec and finally annealing at 72˚C for 10 min. The relative level was calculated using the $2^{-\Delta\Delta Cq}$ method with GAPDH or U6 as the internal reference (21). All the experiments were performed in triplicate and repeated three times. The primer sequences are shown in Table I.

Western blotting. The total proteins in RCC cells or homogenate tissues were isolated using RIPA buffer (Beyotime Institute of Biotechnology) containing PMSF and a protease inhibitor. Protein concentrations were measured using a BCA protein assay kit (Beyotime Institute of Biotechnology). Later, 50 μg of protein sample was loaded on 10% SDS-PAGE and transferred on PVDF membranes at 300 mA. Nonspecific antigens on PVDF membranes were blocked by immersing in TBST (1% Tween) containing 5% skimmed milk in room temperature for 1 h. After immunoblotting with primary antibodies (1:1,000) at 4˚C overnight and secondary antibodies (1:1,000) at room temperature for 1 h. Finally, the membrane was treated with chemiluminescent horse radish peroxidase (HRP) substrate (cat. no. WBKLS0500; MilliporeSigma) to visualize the protein bands and exposure was performed using a Bio-Rad Universal Hood II Gel Doc Imaging system (Bio-Rad Laboratories, Inc.) and the grey value was analyzed using ImageJ 1.8.0.112 (National Institutes of Health). The antibodies used in this study were purchased from ABclonal Biotech Co., Ltd. and the catalog numbers were: UBE2C (cat. no. A5499), AKT (cat. no. A17909), phosphorylated (p)-AKT (cat. no. AP0140), CDK1 (cat. no. A0220), p-CDK1 (cat. no. AP0016), CDK6 (cat. no. A16357), p-CDK1 (cat. no. AP0326), GAPDH (cat. no. A19056) and the secondary antibody HRP Rabbit Anti-Goat IgG (H+L) (cat. no. AS029).

Hematoxylin & Eosin (H&E) staining. RCC specimens were fixed in 4% paraformaldehyde for 24 h at room temperature and dehydrated and transparentized with gradient concentrations (30, 50, 75, 95 and 100%) of ethanol and xylene, and then embedded in paraffin at 55˚C to prepare 4-μm tissue sections for preparing tissue sections. Later, the sections were incubated in xylene (20 min x2), anhydrous ethanol (5 min x2) and 75% ethanol (5 min x1). After washing in ddH$_2$O, the sections were stained using the H&E staining kit (Sangon Biotech Co., Ltd.; cat. no. E607318). Briefly, the sections were stained with hematoxylin for 5 min. After differentiation and bluing, the sections were washed in ddH$_2$O, dehydrated in 85 and 5% ethanol sequentially and stained with eosin for 5 min. All the staining was carried out in a room temperature. Finally, they were incubated in anhydrous ethanol for three times, xylene twice and mounted using neutral gum for observation under a light microscope (XSP-8CA; Shanghai Optical Instrument Co. Ltd.), five fields of view were randomly selected for each tissue section and observed at x100 magnification.

Immunohistochemistry (IHC). The RCC sections were incubated in xylene (15 min x3), dehydrated in anhydrous ethanol (5 min x2), 85% ethanol (5 min x1) and 75% ethanol (5 min x1) and washed in ddH$_2$O. Antigen retrieval was performed by pouring citrate buffer (pH 6.0; Sangon Biotech Co., Ltd.; cat. no. E673000) on the sections at room temperature for 15 min. After incubation in 3% H$_2$O$_2$ in the dark at 37˚C for 25 min and blocking in 3% BSA (Sangon Biotech Co., Ltd.; cat. no. E661003) at 37˚C for 30 min, the sections were incubated with primary antibodies at 4˚C overnight. On the next day, they were washed in PBS (pH 7.4, 5 min x3) and incubated with HRP-labeled secondary antibodies at room temperature for 2 h. Later, the sections were counterstained with DAB and hematoxylin at room temperature for 3 min. After dehydration in ddH$_2$O, 75% ethanol (5 min x1), 85% ethanol (5 min x1), anhydrous ethanol (5 min x2) and *n*-butanol (5 min x1)

sequentially and permeabilization in xylene (5 min x1) at room temperature, neutral gum was used for mounting. The positive staining of cells was observed under a light microscope (XSP-8CA; Shanghai Optical Instrument Co. Ltd.), five fields of view were randomly selected for each tissue section and observed at x100 magnification. The antibodies used in this experiment were purchased from ABclonal Biotech Co., Ltd. and the catalog numbers were: UBE2C (cat. no. A5499) and the secondary antibody (cat. no. AS029).

Lentivirus infection. The GV367 plasmid (Shanghai GeneChem Co., Ltd.) was cut by *Age*I/*Nhe*I and then the FTX sequence or short hairpin (sh)FTX, shUBE2C1, shUBE2C2, shUBE2C3 sequences were spliced to produce overexpressed lentivirus plasmids GV367-FTX and knocked down plasmids GV367-shFTX (Shanghai GeneChem Co., Ltd.), while the non-spliced GV367 was used as a blank control (sequences were as listed: shFTX: 5'-CTGCTACGACAC TGAATTC-3'; shUBE2C1: 5'-CCTGCAAGAAACCTACTC AAA-3'; shUBE2C2: 5'-CTTCTAGGAGAACCCAACA-3'; shUBE2C3: 5'-TGATGTCAGGACCATTCT-3'; and the shNC: 5'-AATTCTCCGAACGTGTCACGT-3'.). Lentivirus packaging was performed using the second-generation lentivirus packaging kit (GeneChem) at 37°C 15 min. The lentiviral plasmid, packaging vector and envelope vector were mixed at a 4:3:2 ratio for a total DNA mass of 20 μg and incubated with 1 ml of Lenti-Easy Packaging Mix (Shanghai GeneChem Co., Ltd.) at 37°C for 15 min. The mixture was then incubated for another 20 min in Lipofectamine® 2000 (Invitrogen; Thermo Fisher Scientific, Inc.) and applied to a 293T cell culture medium for 6 h at 37°C. 293T cells were seeded in a 12-well plate at a density of 2.5×10^5 cells/well and cultured to 80% of confluence. Following the incubation in serum-free DMEM for 4 h, the cells were transfected as mentioned above with lentiviruses at 37°C for 3 days. The transfected cells were filtered using a 0.45 μM mesh, which were concentrated by ultracentrifugation at 70,000 x g at 4°C for 2 h. The supernatant was collected for detecting viral titers. The A498 and A704 cell lines were cultured to over 80% of confluence were cultured with diluted lentiviruses at a multiplicity of infection of 5 and with polybrene (MilliporeSigma) for 24 h and then fresh culture medium was then used to replace the old medium and the GFP-labeled cells with lentivirus transfection rate >80% at 72 h were screened out, stable expressing clones were selected using 4 μg/ml puromycin. The transfection efficacy of lncRNA FTX was finally verified by RT-qPCR as described above.

Measurement of intracellular reactive oxygen species (ROS). To measure intracellular ROS, cells were stained with DCF-DA and subjected to FACS analysis. Cells were plated in 6-well plates at $1.2\text{-}2.0 \times 10^5$ cells/well depending on the proliferation rate of the cell line. After 24 h of incubation, the cells were treated with vehicle (DMSO) or varying concentrations of CDODA-Me (0.5, 1, 2.5, or 5 μM) at 37°C for 3 h and CDODA-Me-induced intracellular ROS were estimated by adding 10 μM DCF-DA.

Inhibition of ROS inductions by GSH was determined by pretreatment with 5 mM GSH for 3 h alone and then in combination with 2.5 μM CDODA-Me at 37°C for 3 h. Cells were then incubated with 10 μM DCF-DA at 37°C for 30 min (at 2 h and 30 min to 3 h treatment time point) at 37°C. Attached and floating cells were then harvested by trypsinization and pelleted by centrifugation at 3,500 x g at 4°C for 5 min. The cells were then resuspended in ice-cold PBS and DCF-DA fluorescence was detected using the FL1 channel of an FC500 flow cytometer (FACSCalibur; BD Biosciences). All experiments were performed in triplicate; data were analyzed using Cell Quest software version (Molecular Devices, LLC, version 5.1) and were shown as means ± SEMs.

Colony formation assay. Cells were seeded in a 6-well plate at a density of 5×10^2 cells/well and cultured for 15 days. Visible colonies were fixed in 4% paraformaldehyde and stained using 0.2% crystal violet at 37°C. The number of colonies (>50 cells) in three replicates per sample was calculated. Images of colonies were captured under an inverted microscope.

MTT assay. The cells were seeded in a 96-well plate at a density of 3×10^3 cells/well in 200 μl of DMEM. Briefly, 15 μl of MTT solution (15 mg/ml, Sangon Biotech Co., Ltd.; cat. no. A600799) was added at 6, 12, 18, 24, 30 and 36 h for 4-h cell culture at 37°C. After lysing in 150 μl of DMSO for 10 min at room temperature, the optical density at 490 nm was measured using an HBS-1101 microplate reader (DeTie).

Flow cytometry for detecting cell cycle progression. The cell cycle progression in RCC cells was measured using a Cell Cycle Staining kit (Sangon Biotech Co., Ltd.; cat. no. E607212). Briefly, the cells were washed in PBS, fixed in 70% ice-cold ethanol and incubated using a commercial kit in the dark at room temperature for 30 min. Cell cycle progression was measured using FC500 flow cytometer (FACSCalibur; BD Biosciences) and analyzed using FlowJo v10 (FlowJo LLC).

Wound healing assay. The A498 and A704 cells were seeded in a 12-well plate at a density of 1×10^5 cells/well. A 1 ml sterile pipette tip was used to make an artificial wound on a cell monolayer and then FBS-free DMEM was replaced. At 0, 12 and 24 h, cell migration was observed using an inverted microscope and assessed by calculating the cell-free zone using ImageJ 1.8.0.112 software (National Institutes of Health, Bethesda).

Transwell assay. Matrigel (Corning Life Sciences; cat. no. 354234) diluted in serum-free DMEM at a ratio of 1:5 was precoated on the Transwell insert at 37°C and dried for 4 h. Cell suspension was prepared in serum-free DMEM at 1×10^5 cells/ml and 200 μl of suspension was added on the top chamber and 500 μl of DMEM containing 10% FBS was added on the bottom. After cell culture for 24 h, the cells on the top chamber were wiped off using a cotton swab. The penetrating cells were fixed in 4% paraformaldehyde at room temperature for 20 min and stained using crystal violet at room temperature for 10 min. After washing and air drying, the cells were observed under a light microscope (XSP-8CA; Shanghai Optical Instrument Co. Ltd.) and the migratory cells were calculated in five randomly selected fields per well.

Dual-luciferase reporter assay. The targeting relationship was predicted by StarBase 3.0 (https://starbase.sysu.edu.cn/) and TargetScan 7.1 (https://www.targetscan.org/vert_71/). Complementary sequences in the UBE2C 3'UTR and promoter region of lncRNA FTX were amplified and cloned in pGL3 3'UTR (Shanghai GeneChem Co., Ltd.) to construct the wild-type (WT) plasmid pGL3-UBE2C-WT, while the mutant-type (Mut) plasmid pGL3-UBE2C-Mut was constructed using a site-directed mutagenesis kit (Sangon Biotech Co., Ltd.; cat. no. B639281). WT plasmid pGL3-FTX-WT and Mut plasmid pGL3-FTX-Mut were similarly constructed. The aforementioned vectors were mixed with the mimics or mimic-NC and Lipofectamine® 2000 (Invitrogen; Thermo Fisher Scientific, Inc.) for 20 min at room temperature. Then, the cells were cotransfected with wild-type/mutant-type plasmid and miR-4429-mimics/mimics-NC, respectively, at 37°C in a humidified atmosphere containing 5% CO_2 for 48 h, the plasmids was transfected at 500 ng per well and the final concentration of mimic or mimic-NC was 20 nM. Relative Firefly and *Renilla* luciferase activities were measured using a Dual-Luciferase Reporter Gene Assay kit (Promega Corporation). Relative luciferase activity was expressed as the ratio of firefly luciferase activity to *Renilla* luciferase activity.

Xenograft model of RCC in nude mice. A total of 18 BALB/c male nude mice (5-6 weeks old; ~15 g; Guangdong Medical Laboratory Animal Center) were habituated in a specific pathogen-free (SPF) environment with 12-h light/dark cycle, at 22±2°C and in a humidity 30-70%. They had free access to food and water. A suspension of RCC cells in PBS ($1x10^8$ cells/ml) was prepared. Prior to inoculation, the cell suspension was mixed with Matrigel (Corning Life Sciences; cat. no. 354234) at a ratio of 1:1 and then 100 μl of mixture was subcutaneously injected into the mouse lateral abdomen. At four weeks later, the mice were sacrificed to collect the subcutaneous tumors. When the mice quickly lost >20% of their original body weight, could not eat and drink, exhibited mental depression with hypothermia, experienced body organ infection or severe liver failure, the experiment was halted and the animals sacrificed. On day 30, a total of 18 mice were sacrificed and no mice succumbed during the experiment. The mice were sacrificed by intraperitoneal injection of sodium pentobarbital with an injection dose of 200 mg/kg. According to AVMA Guidelines for the Euthanasia of Animals: 2020 Edition, the death was confirmed by checking that their hearts had stopped beating for 10 min and the respiratory arrest was also observed. Their size was measured and they were weighed and prepared for the following experiments. The experiments were approved by Ethics Review Committee of Scientific Research of Gannan Medical College (approval number 2020075).

Statistical analyses. Statistical analysis was performed using GraphPad Prism 8 (GraphPad Software, Inc.). Data were normally distributed and are presented as the mean ± SEM. Comparisons between multiple groups were analyzed using one-way ANOVA followed by Tukey's post hoc test or Bonferroni correction. All experiments were performed in triplicate and repeated three times. $P<0.05$ was considered to indicate a statistically significant difference.

Results

lncRNA FTX and UBE2C are upregulated in RCC specimens and cell lines. A total of six pairs of RCC and paracancerous specimens were examined for the expression levels of lncRNA FTX and UBE2C. RT-qPCR data showed that lncRNA FTX and UBE2C mRNA expression were significantly upregulated in RCC specimens than that of paracancerous specimens (Fig. 1A and B). In addition, IHC data showed a significantly higher positive expression of UBE2C in RCC specimens than paracancerous specimens (Fig. 1C). Their expression levels were further detected in RCC cell lines. Consistently, the mRNA level of lncRNA FTX and UBE2C was significantly higher in RCC cell lines compared with those of human renal fibroblast cell line KFB and human proximal convoluted tubular cell line HK-2 (Fig. 1D and E). The protein level of UBE2C was also upregulated in RCC cell lines (Fig. 1F). Collectively, lncRNA FTX and UBE2C were significantly upregulated in RCC specimens and cell lines, indicating their potential roles in the development of RCC.

lncRNA FTX promotes the proliferation, viability, cell cycle progression, migration and invasion of RCC cells. After intervening lncRNA FTX by lentivirus transfection, the malignant phenotypes of RCC cells were evaluated. First, the transfection efficacy of lentivirus was validated by RT-qPCR (Fig. 2A). A colony formation assay proved that the overexpression of lncRNA FTX significantly enhanced the proliferative capacity of RCC cells (Fig. 2B). In addition, the overexpression of lncRNA FTX increased the RCC cell viability as revealed by the MTT assay (Fig. 2C). Compared with those of controls, the cell ratio in G_0/G_1 phase was significantly reduced, while that in G_2/M phases increased, in RCC cells overexpressing lncRNA FTX, indicating that the overexpression of lncRNA FTX significantly accelerated the cell cycle progression of RCC (Fig. 2D). Wound healing assay and Transwell assay results showed the role of lncRNA FTX in promoting the migratory and invasive capacities (Fig. 3A and B). While the intracellular ROS test showed that there are no significantly differences among the groups that treated by lentivirus (Fig. 3C). These data indicated that lncRNA FTX served as an oncogene that promoted the proliferation, viability, cell cycle progression, migration and invasion of RCC cells.

lncRNA FTX exerts the miRNA sponge effect on miR-4429 to upregulate UBE2C. As predicted using the online tools StarBase 3.0 and TargetScan 7.1, a binding site exists between lncRNA FTX and miR-4429 and another binding site exists between miR-4429 and UBE2C 3'UTR (Fig. 4A). A dual-luciferase reporter assay validated that lncRNA FTX could specifically bind to miR-4429 and the latter could specifically bind to its downstream target UBE2C (Fig. 4B and C). The overexpression of lncRNA FTX significantly downregulated miR-4429 and upregulated UBE2C in RCC cells (Fig. 4D-G). Notably, the transfection of miR-4429-mimics could significantly downregulate the expression of UBE2C and effectively reverse the effects on UBE2C of overexpressed lncRNA FTX (Fig. 4H-J). The results showed that lncRNA FTX could bind with miR-4429 and miR-4429 could directly bind with the 3'-UTR sequence of UBE2C and the above results suggested
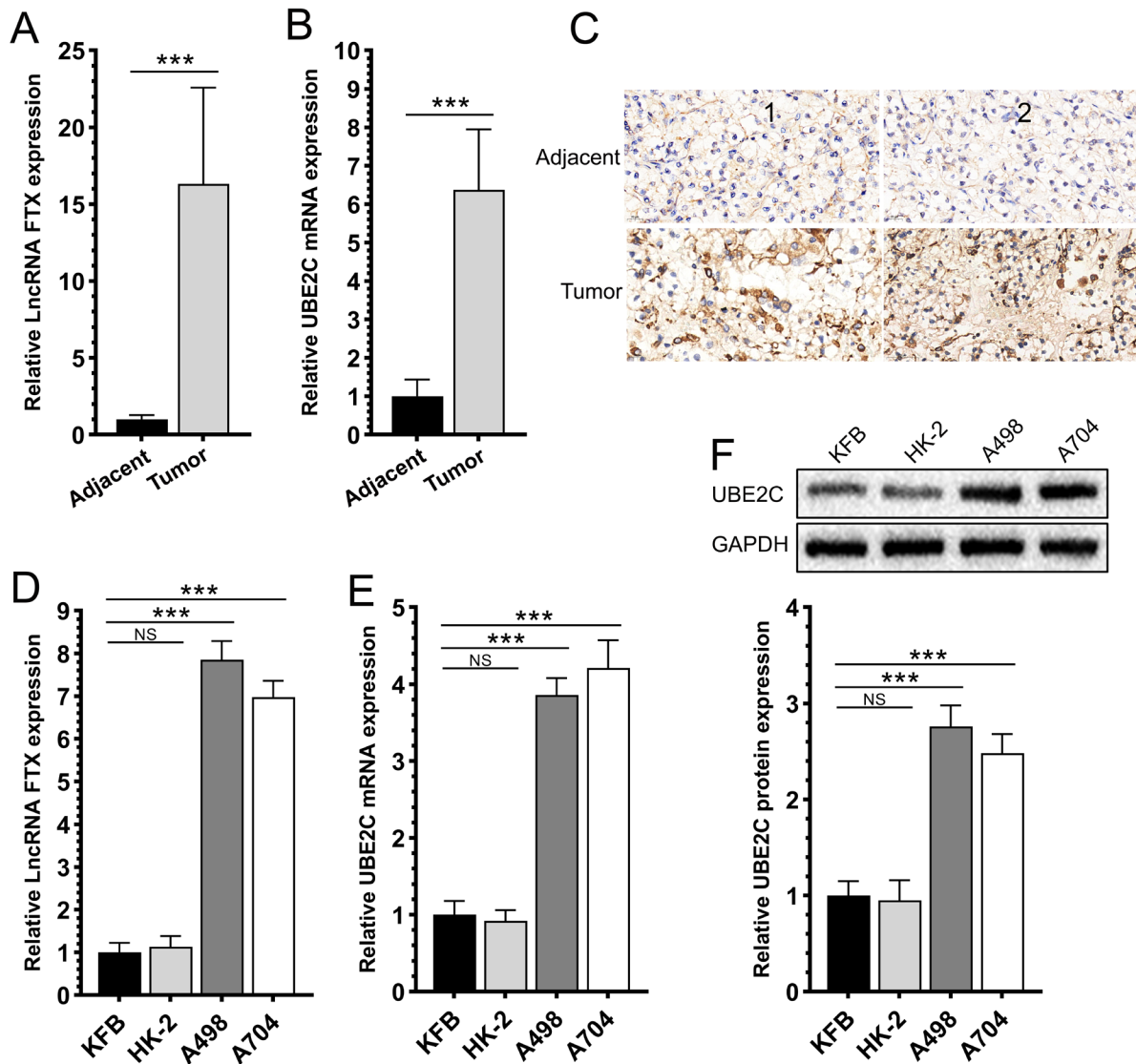
Figure 1. LncRNA FTX and UBE2C are upregulated in RCC specimens and cell lines. (A) Relative lncRNA FTX expression in tumor and adjacent tissues of patients. (B) Relative UBE2C mRNA expression in tumor and adjacent tissues; (C) UBE2C expression in tumor and adjacent tissues (magnification, x100; 1 and 2 are different tissue samples). (D) Relative lncRNA FTX expression in RCC cell lines. (E) Relative UBE2C mRNA expression in RCC cell lines. (F) UBE2C protein expression in RCC cell lines. ***$P<0.001$; NS, not significant; lncRNA, long non-coding RNA; UBE2C, ubiquitin-conjugating enzyme E2C; RCC, renal cell carcinoma.

that there is a signaling lncRNA FTX/miR-4429/UBE2C in RCC.

Knockdown of UBE2C effectively reverses the role of lncRNA FTX in promoting the malignant phenotype of RCC cells. shUBE2C-1, shUBE2C-2, shUBE2C-3 and shNC were synthesized and their transfection efficacies were detected. RT-qPCR and western blotting confirmed the best transfection efficacy of shUBE2C-2 (Fig. 5A and B). Subsequently, the RCC cells were co-transfected with si-UBE2C-2 and overexpression plasmid of lncRNA FTX. A series of functional experiments further indicated that the knockdown of UBE2C effectively reversed the enhanced proliferative, migratory and invasive capacities, viability and accelerated the cell cycle progression in RCC cells overexpressing lncRNA FTX (Figs. 5C-E and 6A and B). In addition, the expression of lncRNA FTX, miR-4429, UBE2C and the upregulated phosphorylation levels of AKT,

CDK1 and CDK6 by the overexpression of lncRNA FTX were downregulated by the knockdown of UBE2C (Fig. 7A and B). It was suggested that lncRNA FTX promoted the progression of RCC by exerting the miRNA sponge effect on miR-4429, thus upregulating UBE2C.

lncRNA FTX significantly affects the size and differentiation of subcutaneous RCC in nude mice. A-498 cells with lncRNA FTX overexpression or knockdown by lentivirus transfection were first subjected to RT-qPCR for validating the transfection efficacy (Fig. 8A). The transfected A-498 cells cultured to 80% confluence were subcutaneously injected into nude mice. The mice were sacrificed at day 30 for collecting tumor tissues. Compared with those of controls, the subcutaneous tumor tissues were larger and heavier in mice implanted with A-498 cells overexpressing lncRNA FTX, while those with lncRNA FTX knockdown had smaller and lighter subcutaneous tumor
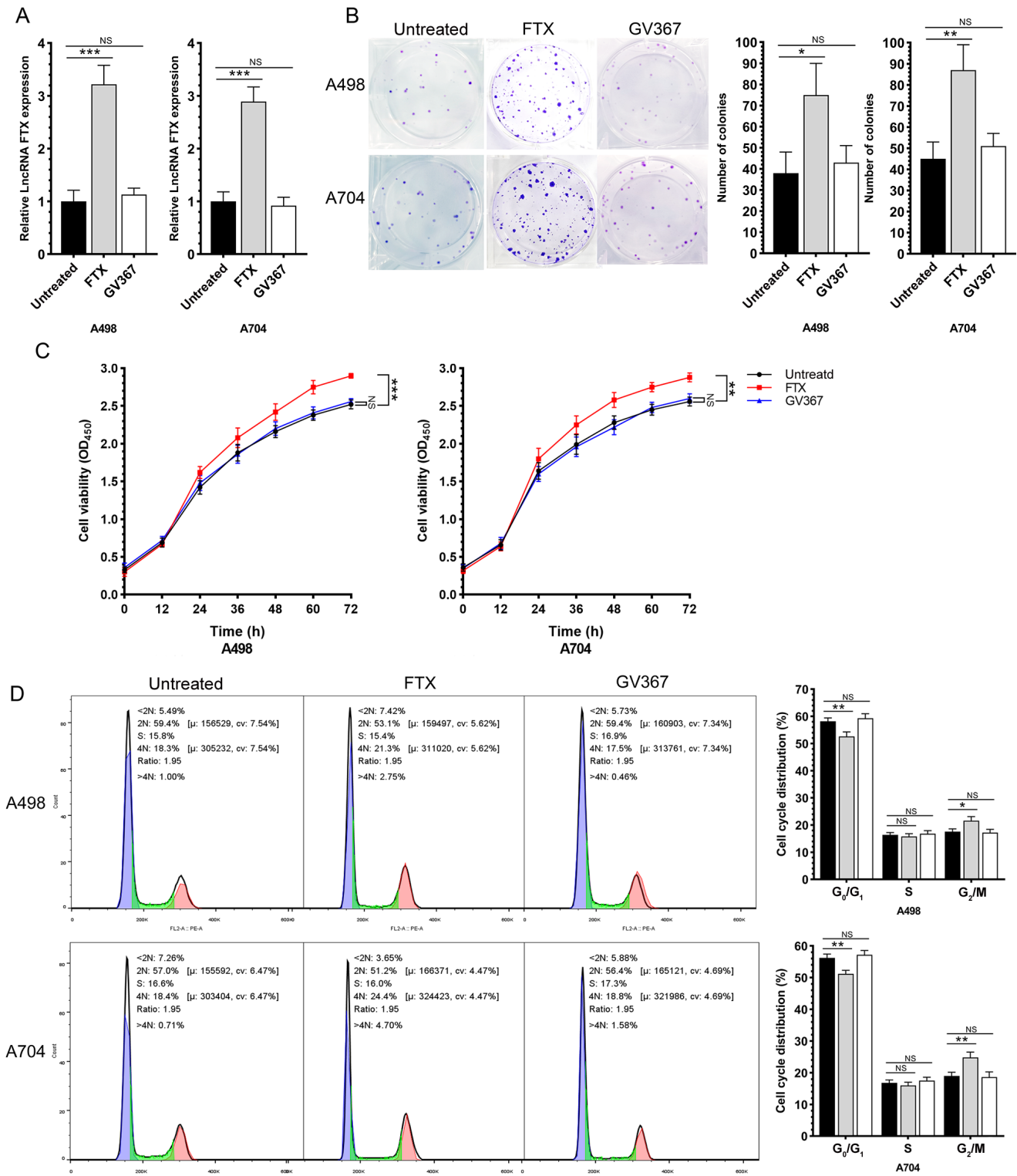
Figure 2. LncRNA FTX promotes the proliferation, viability and cell cycle progression of RCC cells. (A) Transfection efficiency of lentivirus. (B) Cell proliferation of RCC cell lines that overexpressed FTX. (C) Cell viability of RCC cell lines that overexpressed FTX. (D) Cell cycle distribution of RCC cell lines that overexpressed FTX. *P<0.05; **P<0.01; ***P<0.001; NS, not significant; RCC, renal cell carcinoma; FTX long non-coding RNA FTX.

tissues (Fig. 8B and C). Tumor tissues were then prepared for sections and isolation of the total RNA and protein. It was found that the mRNA levels of lncRNA FTX and UBE2C were upregulated and miR-4429 was downregulated in subcutaneous tumor tissues collected from mice implanted with A-498 cells overexpressing lncRNA FTX. The mRNA

and protein levels of UBE2C were upregulated. In mice implanted with A-498 cells with lncRNA FTX knockdown, downregulated UBE2C was detected in subcutaneous tissues (Fig. 8D-H). It was concluded that the *in vivo* overexpression of lncRNA FTX significantly influenced the expression level of UBE2C and the phosphorylation of AKT and CDK6 in
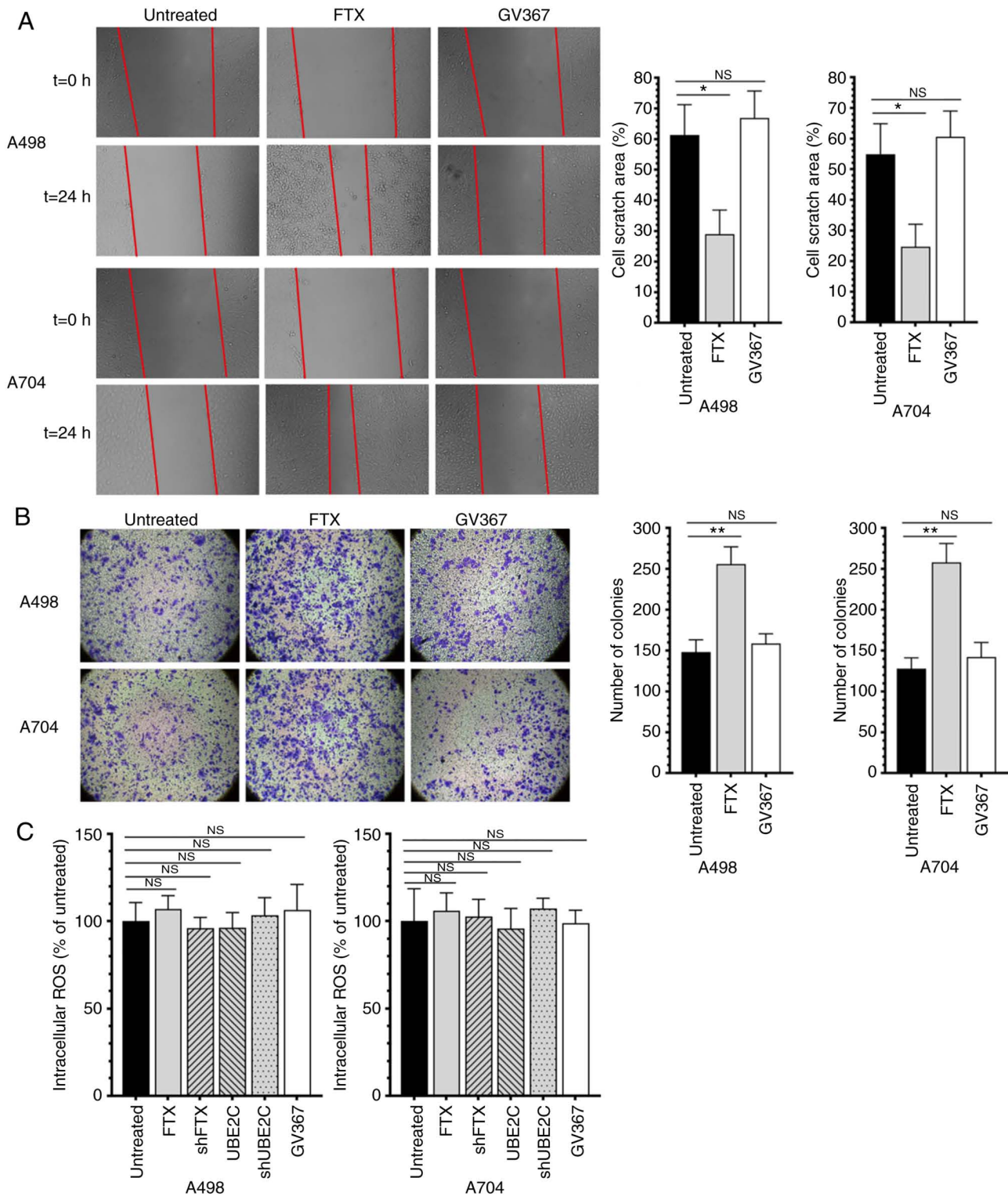
Figure 3. LncRNA FTX promotes the migration and invasion of RCC cells. (A) Migration ability of RCC cell lines that overexpressed FTX (magnifica-tion, x100). (B) Invasive ability of RCC cell lines that overexpressed FTX (magnification, x100). (C) Intracellular ROS level of RCC cell lines treated by lentivirus. *P<0.05; **P<0.01; NS, not significant; RCC, renal cell carcinoma; FTX long non-coding RNA FTX; ROS, reactive oxygen species; t, time.

tumor tissues, accelerating the carcinogenesis by implanting A-498 cells in nude mice.

Discussion

RCC is a globally prevalent type of cancer. More than 140,000 deaths of RCC are reported every year, ranking 13th among

the cancer mortality in the world (22). Although the early nonmetastatic RCC can be surgically treated, the recurrence rate of RCC is ≤40%. Metastatic RCC has a poor prognosis and low survival rate (23). Novel biomarkers for RCC micro-environment and immunotherapy have been widely analyzed. Targeted drugs including sunitinib (24) and bevacizumab (25) that inhibit VEGF and its receptor VEGFR, sirolimus (26) that

A

LncRNA FTX (chrX: 7399926-73499945):   5′ ...UAUUGUCGAUGG**CAGCUUU**C... 3′

miRNA-4429:   3′   GCGGAGAGUCGG**GUCGAAAA**   5′

Position 34-40 of UBE2C 3′-UTR: 5′ ...UCUGGAAAAACCCCA**CAGCUUUU**... 3′

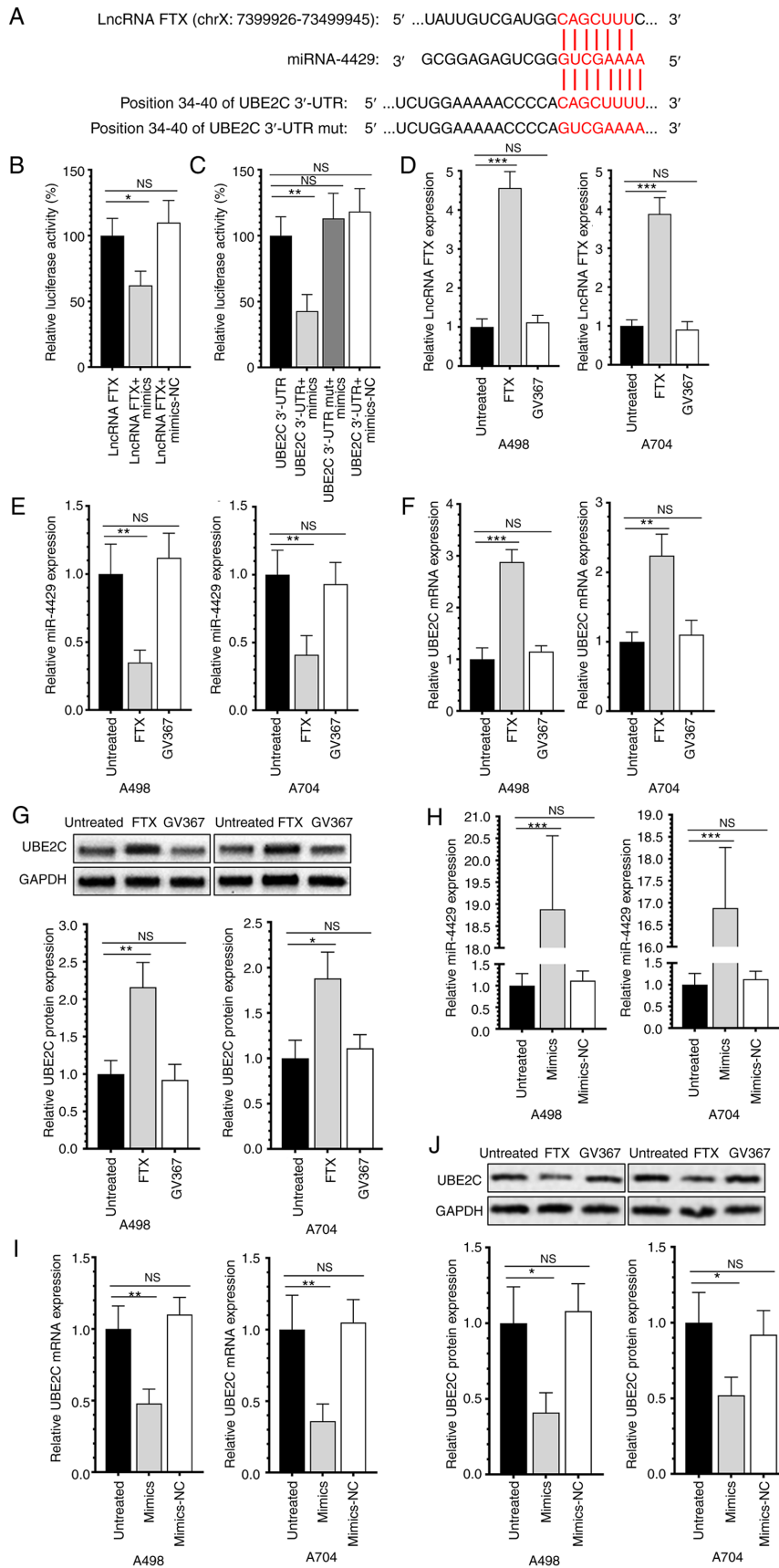Position 34-40 of UBE2C 3′-UTR mut: 5′ ...UCUGGAAAAACCCCA**GUCGAAAA**... 3′

Figure 4. LncRNA FTX exerts the miRNA sponge effect on miR-4429 to upregulate UBE2C. (A) Prediction of the relevance among lncRNA FTX, miR-4429 and UBE2C; (B) Double luciferase activity detection between lncRNA FTX and miR-4429; (C) Double luciferase activity detection between miR-4429 and UBE2C; (D) Transfection efficiency of lentivirus that overexpress FTX; (E) Relative miR-4429 expression in RCC cell lines that overexpressed FTX; (F) Relative UBE2C mRNA expression in RCC cell lines that overexpressed FTX; (G) UBE2C expression in RCC cell line that overexpressed FTX; (H) Transfection efficiency of miR-4429 mimics; (I) Relative UBE2C mRNA expression in RCC cell lines transfected with miR-4429 mimics; (J) UBE2C expression in RCC cell line transfected with miR-4429 mimics. *P<0.05; **P<0.01; ***P<0.001; NS, not significant; lncRNA, long non-coding RNA; miR, microRNA; UBE2C, ubiquitin-conjugating enzyme E2C; RCC, renal cell carcinoma; NC, negative control.
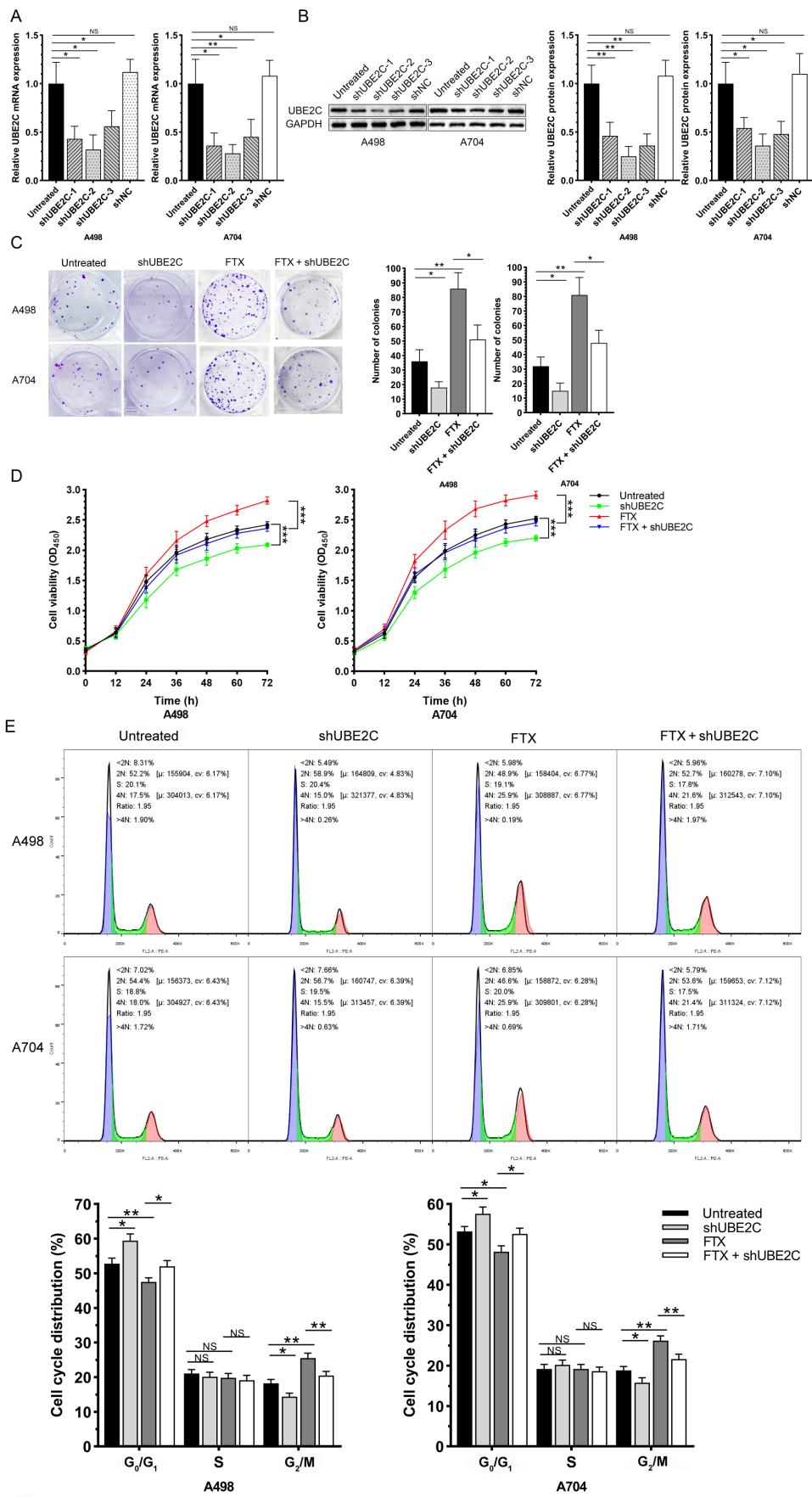
Figure 5. Knockdown of UBE2C effectively reverses the role of lncRNA FTX in the proliferation, viability, and cell cycle progression of RCC cells. (A) Transfection efficiency of lentivirus. (B) UBE2C expression of RCC cell lines. (C) Colony formation of RCC cell lines that overexpressed FTX or knocked down UBE2C. (D) Cell viability of RCC cell lines that overexpressed FTX or knocked down UBE2C. (E) Cell cycle distribution of RCC cell lines that overexpressed FTX or knocked down UBE2C. *P<0.05; **P<0.01; ***P<0.001; NS, not significant; UBE2C, ubiquitin-conjugating enzyme E2C; RCC, renal cell carcinoma; FTX long non-coding RNA FTX; sh, short hairpin.
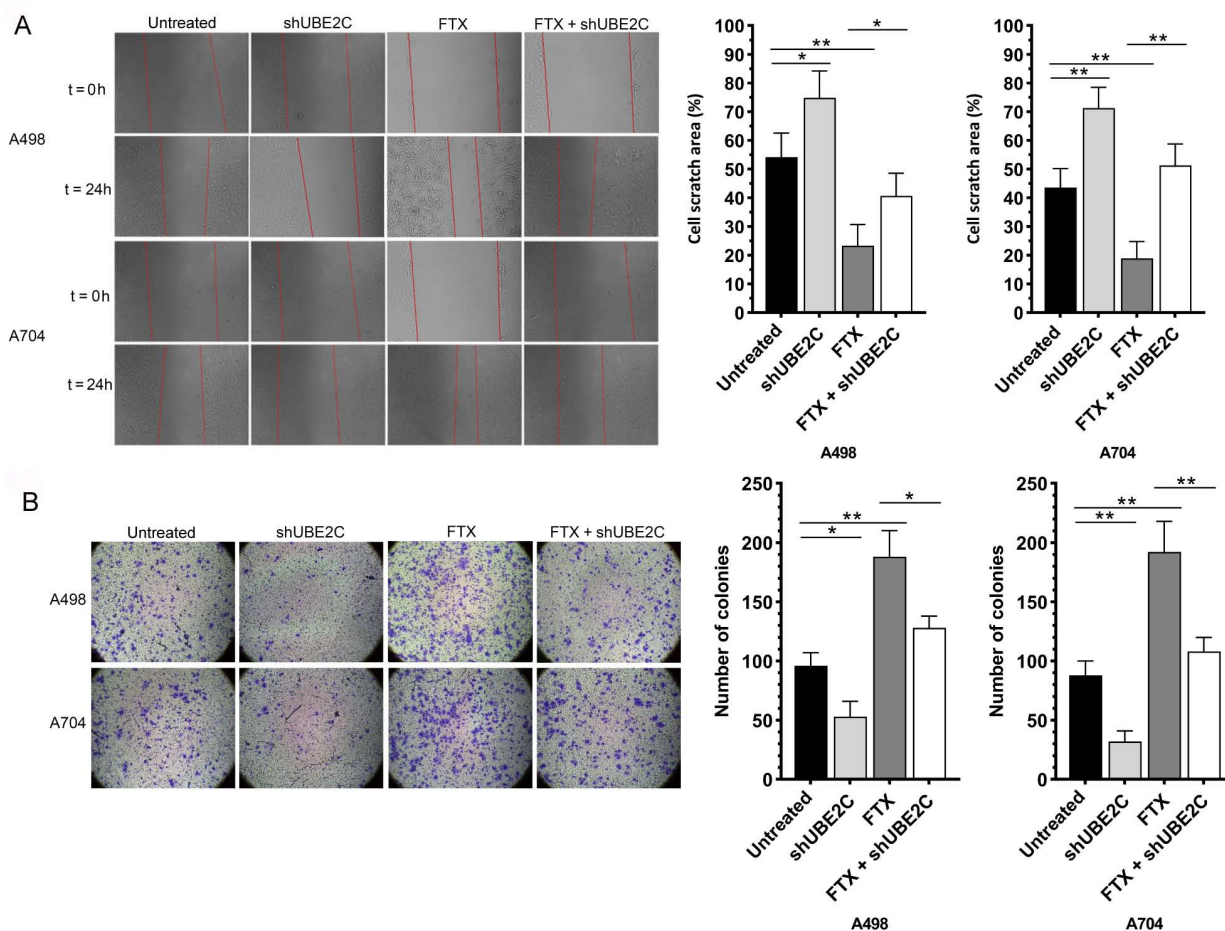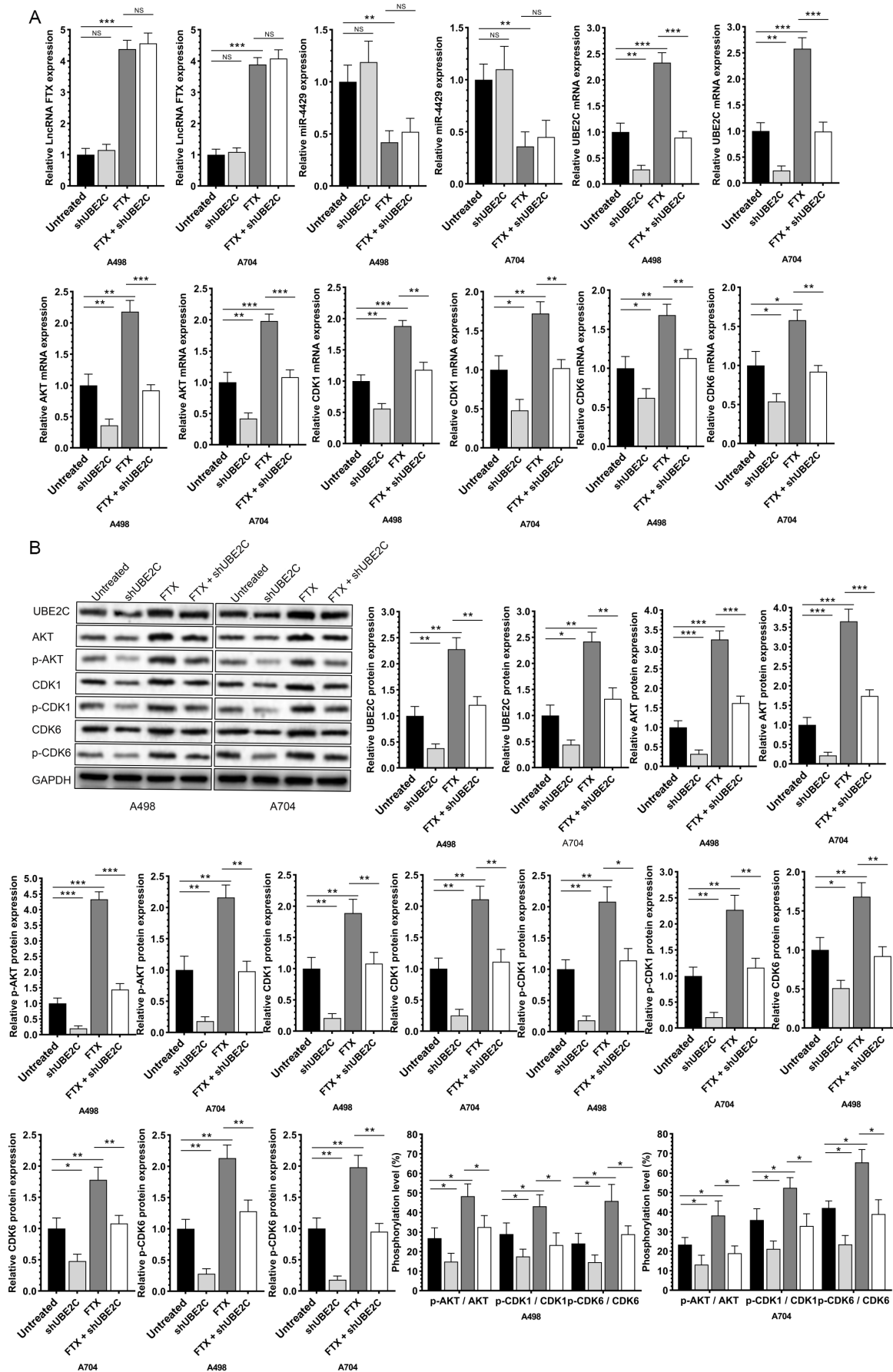
Figure 6. Knockdown of UBE2C effectively reverses the role of lncRNA FTX in the migration and invasion of RCC cells. (A) Migration ability of RCC cell lines that overexpressed FTX or knocked down UBE2C (magnification, x100); (B) Invasive ability of RCC cell lines that overexpressed FTX or knocked down UBE2C (magnification, x100). *P<0.05; **P<0.01; NS, not significant; RCC, renal cell carcinoma; FTX long non-coding RNA FTX; UBE2C, ubiquitin-conjugating enzyme E2C; t, time.

inhibits mTOR and nivolumab (27) used in immune therapies have been used for the treatment of metastatic RCC. It is important to actively search for new biomarkers and therapeutic targets of RCC.

lncRNA FTX has been extensively evaluated as a vital regulator of cancer cells. Chen *et al* (28) report that FTX is abnormally overexpressed in osteosarcoma (OS) tissues and cells that promote the proliferation and invasion and inhibits the apoptosis of OS cells by regulating the miR-214-5p/SOX4 axis, indicating that FTX might be a potential therapeutic target for OS. Zhao *et al* (29) show that lncRNA FTX promotes the progression of colorectal cancer (CRC) by regulating the miR-192-5p/EIF5A2 axis as an oncogene, providing new insights into the pathogenesis of CRC. Jin *et al* (30) reveal a novel ceRNA axis FTX/miR-200a-3p/FOXA2 in lung cancer cells, validating the therapeutic potential of FTX in lung cancer. In addition, FTX is upregulated in liver cancer, RCC, glioma and hematological cancer (31) and the regulatory effects of FTX on the invasion and migration of RCC cells has been confirmed (17). The present study consistently showed the presence of upregulated lncRNA FTX in RCC specimens. In addition, it showed that the overexpression of lncRNA FTX promoted the proliferation, cell cycle progression, migration and invasion of RCC cells and upregulated UBE2C, p-AKT,

p-CDK1 and p-CDK6. In addition, the *in vivo* overexpression of lncRNA FTX in RCC cells significantly enlarged the size and increased the weight of subcutaneous tissues in nude mice. Taken together, the findings demonstrated the vital function of lncRNA FTX in aggravating the progression of RCC.

miRs have been previously confirmed to regulate the expression levels of RCC-related proteins, which serve as effective biomarkers for diagnosing, accurately determining the molecular classification and predicting the prognosis of RCC (32). miR-4429 is widely involved in the progression of various types of tumors. Wang *et al* (33) found that miR-4429 inhibits the growth of prostate cancer cells by downregulating DLX1 and inactivating the Wnt/β-catenin pathway. Li *et al* (34) demonstrated that miR-4429 blocks the proliferation, migration, invasion and epithelial-mesenchymal transition (EMT) process of CRC cells by targeting FOXM1 to downregulate SMAD3. Cai *et al* (35) confirm that the silencing of lncRNA SNHG12 and overexpression of miR-4429 significantly inhibit the proliferation, migration and invasion of RL95-2 cells by downregulating MMP2 and MMP9 and targeting of the SNHG12/miR-4429 axis and can be used as a potential therapeutic target for endometrial cancer in the future. Pan *et al* (36) also report that miR-4429 suppresses ccRCC tumor progression and EMT by targeting CDK6. The present

Figure 7. Knockdown of UBE2C effectively reverses the role of lncRNA FTX in gene expression of RCC cells. (A) Relative RNA expression of RCC cell lines that overexpressed FTX or knocked down UBE2C; (B) Relative proteins expression of RCC cell lines that overexpressed FTX or knocked down UBE2C. *P<0.05; **P<0.01; ***P<0.001; NS, not significant; RCC, renal cell carcinoma; FTX long non-coding RNA FTX; UBE2C, ubiquitin-conjugating enzyme E2C; p-, phosphorylated; sh, short hairpin.
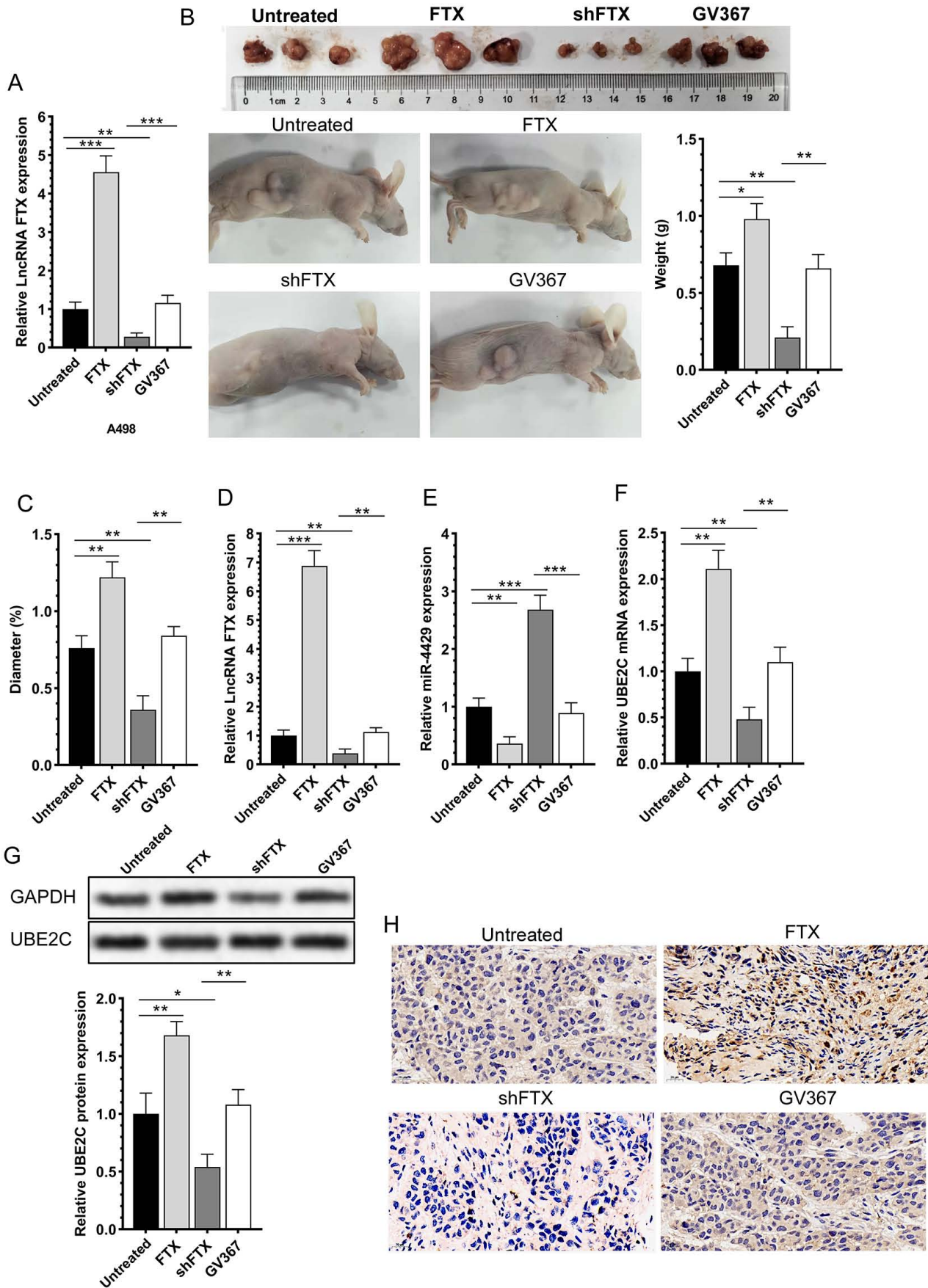
Figure 8. LncRNA FTX significantly affects the size and differentiation of subcutaneous RCC in nude mice. (A) Transfection efficiency of lentivirus; (B) Weight of tumor tissues; (C) Diameter of tumor tissues; (D) Relative lncRNA FTX expression in mice-tumor tissues; (E) Relative miR-4429 expression in mice-tumor tissues; (F) Relative UBE2C mRNA expression in mice-tumor tissues; (G) Relative UBE2C protein expression in mice-tumor tissues; (H) IHC of UBE2C in mice-tumor tissues (magnification, x100). $^{*}P<0.05$; $^{**}P<0.01$; $^{***}P<0.001$; NS, not significant; lncRNA, long non-coding RNA; UBE2C, ubiquitin-conjugating enzyme E2C; sh, short hairpin.

study predicted and later confirmed that lncRNA FTX specifically targeted miR-4429 and the latter could specifically bind to UBE2C 3'UTR using an online tool and dual-luciferase reporter assay, respectively. lncRNA FTX overexpression was able to downregulate miR-4429 and enhance the transcription level of UBE2C. In addition, the overexpression of miR-4429 significantly reversed the promotive effect of lncRNA FTX on the progression of RCC and expression level of UBE2C. It is suggested that the regulatory function of lncRNA FTX in the malignant progression of RCC depends on the miRNA sponge effect on miR-4429 to upregulate UBE2C.

UBE2C has been widely studied in cancers due to its carcinogenic effect. Wang *et al* (37) found that UBE2C is highly expressed in gastric cancer tissues. Silencing of UBE2C not only inhibits the colony formation of gastric cancer cells, but also DNA biosynthesis. In addition, miR-300 inhibits the progression of gastric cancer by reducing the abundance of UBE2C mRNA. Hu *et al* (38) report that the knockdown of UBE2C inhibits the proliferation and invasion of prostate cancer cells, which is a direct target of miR-381-3p. Icaritin downregulates UBE2C and upregulates miR-381-3p in human prostate cancer cells. Zhang *et al* (39) confirm that UBE2C is upregulated in rectal cancer and that the knockdown of UBE2C significantly inhibits the growth of xenograft tumor in mice. Previous studies support the oncogenic role of UBE2C in RCC, although the specific mechanism remains to be elucidated (20,39). The present study also identified upregulated UBE2C in RCC specimens. Notably, the knockdown of UBE2C effectively reversed the promoted proliferation, viability, cell cycle progression, migration and invasion induced by the overexpression of lncRNA FTX, as well as upregulating p-AKT, p-CDK1 and p-CDK6. It is suggested that UBE2C was responsible for aggravating the malignant progression of RCC through the FTX/miR-4429/UBE2C axis. In addition, implantation of A-498 cells overexpressing lncRNA FTX in nude mice resulted in enlarged subcutaneous tissues with heavier tumor weight compared with those of controls. lncRNA FTX also regulated UBE2C, p-AKT, p-CDK1 and p-CDK6 in subcutaneous tissues. Taken together, the *in vivo* findings indicate that lncRNA FTX significantly influenced the UBE2C level and phosphorylation of AKT, CDK1 and CDK6 and promoted the carcinogenesis of implanting A-498 cells in nude mice. The effects of lncRNA FTX in promoting the malignant phenotype of RCC could be significantly reversed by knockdown of UBE2C, which indicated that the axis lncRNA FTX/miR-4429/UBE2C could significantly influence the proliferation, viability, cell cycle progression, migration and invasion of RCC cells and hence are promising biomarkers and therapeutic targets for RCC.

In general, the present study examined the abnormally high expression of lncRNA FTX in RCC, its promoting effects and mechanism on RCC malignant phenotype. The results showed that lncRNA FTX could significantly promote the cell viability, proliferation, migration and invasion of RCC. lncRNA FTX acted as a molecular sponge of miR-4429 and promoted the process of RCC through the FTX/mir-4429/UBE2C axis. However, due to the limited number of the clinical samples, the correlation of clinical data could not be well demonstrated, which might be the main limitation of the present study. In addition, the present study did not test the expression level of apoptosis-related genes, which would be another limitation and a future research perspective.

In brief, lncRNA FTX and UBE2C are significantly upregulated in RCC specimens. Through the miRNA sponge effect on miR-4429 to upregulate UBE2C, lncRNA FTX markedly promoted the proliferation, viability, cell cycle progression, migration and invasion of RCC cells, thus aggravating the malignant progression of RCC. The findings indicated that lncRNA FTX and UBE2C are promising biomarkers and therapeutic targets for RCC.

Availability of data and materials

The datasets used and/or analyzed during the current study are available from the corresponding author on reasonable request.

Authors' contributions

ZC, and LW made substantial contributions to the conception or design of the work and agreed to be accountable for all aspects of the work in ensuring that questions related to the accuracy and integrated of any part of the work are appropriately investigated and resolved. ZC, MZ and YuL performed the experiments. TD, ZL and LW performed the acquisition, analysis, and interpretation of data. TD, YaL and ZZ drafted the manuscript and revised it critically for important intellectual content; ZC and LW confirm the authenticity of all the raw data; all the authors approved the final version to be published.

Ethics approval and consent to participate

This research was approved by the Ethics Review Committee of Scientific Research of Gannan Medical College (approval number 2020075).

Patient consent for publication

Not applicable.

Competing interests

The authors declare that they have no competing interests.

References

1. Padala SA, Barsouk A, Thandra KC, Saginala K, Mohammed A, Vakiti A, Rawla P and Barsouk A: Epidemiology of renal cell carcinoma. World J Oncol 11: 79-87, 2020.
2. Shen H, Luo G and Chen Q: Long noncoding RNAs as tumorigenic factors and therapeutic targets for renal cell carcinoma. Cancer Cell Int 21: 110, 2021.

3. Sun M, Thuret R, Abdollah F, Lughezzani G, Schmitges J, Tian Z, Shariat SF, Montorsi F, Patard JJ, Perrotte P and Karakiewicz PI: Age-adjusted incidence, mortality, and survival rates of stage-specific renal cell carcinoma in North America: A trend analysis. Eur Urol 59: 135-141, 2011.
4. Weyerer V, Strissel PL, Stohr C, Eckstein M, Wach S, Taubert H, Brandl L, Geppert CI, Wullich B, Cynis H, et al: Endogenous Retroviral-K envelope is a novel tumor antigen and prognostic indicator of renal cell carcinoma. Front Oncol 11: 657187, 2021.
5. Tacconi EMC, Tuthill M and Protheroe A: Review of adjuvant therapies in renal cell carcinoma: Evidence to date. Onco Targets Ther 13: 12301-12316, 2020.
6. Hsieh JJ, Purdue MP, Signoretti S, Swanton C, Albiges L, Schmidinger M, Heng DY, Larkin J and Ficarra V: Renal cell carcinoma. Nat Rev Dis Primers 3: 17009, 2017.
7. Maher ER: Hereditary renal cell carcinoma syndromes: Diagnosis, surveillance and management. World J Urol 36: 1891-1898, 2018.
8. Gallan AJ, Parilla M, Segal J, Ritterhouse L and Antic T: BAP1-Mutated clear cell renal cell carcinoma. Am J Clin Pathol 155: 718-728, 2021.
9. Kim BJ, Kim JH, Kim HS and Zang DY: Prognostic and predictive value of VHL gene alteration in renal cell carcinoma: A meta-analysis and review. Oncotarget 8: 13979-13985, 2017.
10. Ciomborowska-Basheer J, Staszak K, Kubiak MR and Makalowska I: Not so dead genes-retrocopies as regulators of their disease-related progenitors and hosts. Cells 10: 912, 2021.
11. Li Q, Tian Y, Hu G, Liang Y, Bai W and Li H: Highly expressed antisense noncoding RNA in the INK4 locus promotes growth and invasion of renal clear carcinoma cells via the β-catenin pathway. Oncol Res 25: 1373-1382, 2017.
12. Wang G, Li H and Hou Y: LncRNA MAGI2-AS3 inhibits tumor progression and angiogenesis by regulating ACY1 via interacting with transcription factor HEY1 in clear cell renal cell carcinoma. Cancer Gene Ther 29: 585-596, 2021.
13. Cheng T, Shuang W, Ye D, Zhang W, Yang Z, Fang W, Xu H, Gu M, Xu W and Guan C: SNHG16 promotes cell proliferation and inhibits cell apoptosis via regulation of the miR-1303-p/STARD9 axis in clear cell renal cell carcinoma. Cell Signal 84: 110013, 2021.
14. Zhang J, Jin S, Xiao W, Zhu X, Jia C and Lin Z: Long noncoding RNA LINC00641 promotes renal cell carcinoma progression via sponging microRNA-340-5p. Cancer Cell Int 21: 210, 2021.
15. Zhang F, Wang XS, Tang B, Li PA, Wen Y and Yu PW: Long non-coding RNA FTX promotes gastric cancer progression by targeting miR-215. Eur Rev Med Pharmacol Sci 24: 3037-3048, 2020.
16. Huo X, Wang H, Huo B, Wang L, Yang K, Wang J, Wang L and Wang H: FTX contributes to cell proliferation and migration in lung adenocarcinoma via targeting miR-335-5p/NUCB2 axis. Cancer Cell Int 20: 89, 2020.
17. He X, Sun F, Guo F, Wang K, Gao Y, Feng Y, Song B, Li W and Li Y: Knockdown of long noncoding RNA FTX inhibits proliferation, migration, and invasion in renal cell carcinoma cells. Oncol Res 25: 157-166, 2017.
18. Hao Z, Zhang H and Cowell J: Ubiquitin-conjugating enzyme UBE2C: Molecular biology, role in tumorigenesis, and potential as a biomarker. Tumour Biol 33: 723-730, 2012.
19. Xie C, Powell C, Yao M, Wu J and Dong Q: Ubiquitin-conjugating enzyme E2C: A potential cancer biomarker. Int J Biochem Cell Biol 47: 113-117, 2014.
20. Chen Z and Wang L: The clinical significance of UBE2C gene in progression of renal cell carcinoma. Eur J Histochem 65: 3196, 2021.
21. Livak KJ and Schmittgen TD: Analysis of relative gene expression data using real-time quantitative PCR and the 2(-Delta Delta C(T)) Method. Methods 25: 402-408, 2001.
22. Capitanio U, Bensalah K, Bex A, Boorjian SA, Bray F, Coleman J, Gore JL, Sun M, Wood C and Russo P: Epidemiology of renal cell carcinoma. Eur Urol 75: 74-84, 2019.
23. Larroquette M, Peyraud F, Domblides C, Lefort F, Bernhard JC, Ravaud A and Gross-Goupil M: Adjuvant therapy in renal cell carcinoma: Current knowledges and future perspectives. Cancer Treat Rev 97: 102207, 2021.
24. Motzer RJ, Hutson TE, Tomczak P, Michaelson MD, Bukowski RM, Rixe O, Oudard S, Negrier S, Szczylik C, Kim ST, et al: Sunitinib versus interferon alfa in metastatic renal-cell carcinoma. N Engl J Med 356: 115-124, 2007.
25. Escudier B, Pluzanska A, Koralewski P, Ravaud A, Bracarda S, Szczylik C, Chevreau C, Filipek M, Melichar B, Bajetta E, et al: Bevacizumab plus interferon alfa-2a for treatment of metastatic renal cell carcinoma: A randomised, double-blind phase III trial. Lancet 370: 2103-2111, 2007.
26. Yang S, de Souza P, Alemao E and Purvis J: Quality of life in patients with advanced renal cell carcinoma treated with temsirolimus or interferon-alpha. Br J Cancer 102: 1456-1460, 2010.
27. Motzer RJ, Escudier B, McDermott DF, Arén Frontera O, Melichar B, Powles T, Donskov F, Plimack ER, Barthélémy P, Hammers HJ, et al: Survival outcomes and independent response assessment with nivolumab plus ipilimumab versus sunitinib in patients with advanced renal cell carcinoma: 42-month follow-up of a randomized phase 3 clinical trial. J Immunother Cancer 8: e000891, 2020.
28. Chen H, Liu T, Ouyang H, Lin S, Zhong H, Zhang H and Yang Y: Upregulation of FTX promotes osteosarcoma tumorigenesis by increasing SOX4 expression via miR-214-5p. Onco Targets Ther 13: 7125-7136, 2020.
29. Zhao K, Ye Z, Li Y, Li C, Yang X, Chen Q and Xing C: LncRNA FTX contributes to the progression of colorectal cancer through regulating miR-192-5p/EIF5A2 axis. Onco Targets Ther 13: 2677-2688, 2020.
30. Jin S, He J, Zhou Y, Wu D, Li J and Gao W: LncRNA FTX activates FOXA2 expression to inhibit non-small-cell lung cancer proliferation and metastasis. J Cell Mol Med 24: 4839-4849, 2020.
31. Lin Y, Sheng Y, Chen J, Hu C, Zhou Z and Yuan C: The function of LncRNA FTX in several common cancers. Curr Pharm Des 27: 2381-2386, 2021.
32. Tsiakanikas P, Giaginis C, Kontos CK and Scorilas A: Clinical utility of microRNAs in renal cell carcinoma: Current evidence and future perspectives. Expert Rev Mol Diagn 18: 981-991, 2018.
33. Wang J, Xie S, Liu J, Li T, Wang W and Xie Z: MicroRNA-4429 suppresses proliferation of prostate cancer cells by targeting distal-less homeobox 1 and inactivating the Wnt/β-catenin pathway. BMC Urol 21: 40, 2021.
34. Li H, Liang W, Zhang H, Shui Y and Zhang Z: MicroRNA-4429 restrains colorectal cancer cell invasion and migration via regulating SMAD3-induced epithelial-mesenchymal transition. J Cell Physiol 236: 5875-5884, 2021.
35. Cai P, Wu M, Zhang B, Wu S, Wei H and Wei L: Long noncoding RNA SNHG12 regulates cell proliferation, invasion and migration in endometrial cancer by targeting miR4429. Mol Med Rep 22: 2842-2850, 2020.
36. Pan H, Hong Y, Yu B, Li L and Zhang X: miR-4429 inhibits tumor progression and epithelial-mesenchymal transition via targeting CDK6 in clear cell renal cell carcinoma. Cancer Biother Radiopharm 34: 334-341, 2019.
37. Wang Y, Huang F, Liu M and Zhao Q: UBE2C mRNA expression controlled by miR-300 and HuR determines its oncogenic role in gastric cancer. Biochem Biophys Res Commun 534: 597-603, 2021.
38. Hu J, Wu X, Yang C, Rashid K, Ma C, Hu M, Ding Q and Jiang H: Anticancer effect of icaritin on prostate cancer via regulating miR-381-3p and its target gene UBE2C. Cancer Med 8: 7833-7845, 2019.
39. Zhang Y, Tian S, Li X, Ji Y, Wang Z and Liu C: UBE2C promotes rectal carcinoma via miR-381. Cancer Biol Ther 19: 230-238, 2018.